*Fibers and Polymers* 2018, Vol.19, No.7, 1567-1575
DOI 10.1007/s12221-018-8033-2

ISSN 1229-9197 (print version)
ISSN 1875-0052 (electronic version)

# A Novel Study on Thermal Stability of Camphor Soot Reinforced Coir Fibers

**T. Raghavendra and Panneerselvam Kavan***

*Department of Production Engineering, National Institute of Technology, Tiruchirappalli 620015, India*
(Received January 16, 2018; Revised May 25, 2018; Accepted May 30, 2018)

**Abstract:** Thermoplastics, reinforced with lignocellulosic fibers are usually processed at lower temperatures ranging from 100 °C to 160 °C. Further increase in temperature leads to the degradation of the fibers mechanical properties. Camphor soot reinforced coir fibers (CSRCF) based on the osmosis technique were prepared, in this study. Parameters using Design of Experiments (DOE) varied and the process is investigated for varied camphor soot concentrations (0.5, 1.0 and 1.5 wt. %), time (4, 8 and 12 hrs.) and temperature (30, 40 and 50 °C) with three levels for each parameter ($L_9$ Orthogonal array). Relative camphor soot content in the coir fiber (RCSCF) and tensile strength are vital objective functions. Tensile tests were conducted on tensometer according to DOE, and based on analysis of variance (ANOVA). The optimal results from ANOVA were established by charting the main effect plots. The optimal combination of parameters for CSRCF were examined using X-ray diffraction (XRD), thermogravimetric analysis (TGA) and Fourier transform infrared radiation (FTIR). Further, scanning electron microscope (SEM) equipped with an energy dispersion spectroscope (EDS) examined and compared neat fibers. The results showed a considerable increase in tensile strength by about 37 % for CSRCF compared to neat fibers. XRD revealed that crystallinity index was slightly reduced for modified fibers. The TGA result reveals that thermal stability of the modified fibers improved by 15 % compared to neat fibers. FTIR analysis revealed that modified fibers experienced peak diminishing in OH, CH stretching and carbonyl groups. The Morphology study of neat and CSRCF were examined using SEM with EDS analysis which revealed 94 % carbonaceous compounds in a cross examination of modified fibers compared to the cross section of a neat coir fiber (64 %).

**Keywords:** Camphor soot, Coir fibers, Osmosis, Thermal stability, Scanning electron microscope

## Introduction

Coir fibers are coarse and thick are, extracted from coconut shells, found in abundance in Asian countries like India, Indonesia, Srilanka, Thailand, Vietnam and Malaysia [1]. Coir fibers are used to create a variety of flooring materials like mattresses, yarns, brushes, rugs, boats, insulation panels and geotextiles. Due to its durability, high stiffness, sound resistance, resistance to fungi and microbial degradation, it has non-flammable, additional resistance to humidity compared to other natural fibers. It is also stable in high temperature and saline water [2,3]. Moreover, coconut trees which have highest osmosis rates due to their gigantic structure results in their fibers highly porous. Coir fibers comprise elementary fibers (in a range of 200 to 300) and a lacuna at the center. The elementary fibers are built up of two main cell walls comprising bundles of microfibrils aligned at an angle to the fiber axis. Coir fibers have a porosity of about 22-30 % [4]. The thermal stability of lignocellulosic fiber is a continuing investigation that researchers anticipate as most natural fibers have low degradation temperature (~200 °C) making them incompatible for processing with thermoplastics with higher melting points [5]. This was problem that motivated investigation in to the thermal stability of lignocellulosic fibers. Though enhancement of lignocellulosic fiber and matrix compatibility has attracted research [6,7], only few works were undertaken on improving natural fibers thermal stability [8]. Zadorecki *et al.* experimented with reaction injection molding to reinforce cellulose in nylon-6. The process used two liquid component systems that were injected into the closed mould, where polymerization occurs at 130 °C to avoid cellulose degradation. They concluded that processing cannot produce composites with high fiber content as viscosity increases rapidly with increased fiber content [9]. Klason *et al.* reported that Cellulose fibers degraded rapidly at processing temperatures beyond 200 °C. The authors stated cellulose fibers failed to produce significant reinforcement in thermoplastics with melting point above 230 °C despite their apparent stiffness and strength [10]. Mishra *et al.* used small quantities of inorganic salts during melt extrusion processing to decrease melting temperatures of nylon 6. Lithium chloride (LiCl) salt was added to nylon 6 during extrusion and it was felt that addition of 5 wt. % LiCl decreased nylon's melting point from 223 to 191 °C and increased both tensile modulus and tensile strength by 275 % and 30 % respectively [11]. These issues could be offset by Interfacial alterations of lignocellulosic fibers which improve the circumstance either by surface treatments, additives, or surface coatings [12]. Conversely, their extensive use in industrial applications is tedious. They are limited by drawbacks such as differing dimensional and structural variations (e.g., diameter, density, length, etc.), hydrophilicity, poor compatibility with polymers and, low thermal sensitivity which have to be overcome [13,14]. Natural fibers affinity to water indicates high rate of humidity absorption, the main reason for poor bonding with hydrophobic polymeric matrices. However, these difficulties

*Corresponding author: kps@nitt.edu

can be offset by alkali chemical treatments [15]. Natural fibers thermal stability can be increased using additives or surface treatments viz. usage of camphor soot as it is thermally stable and acts as a reinforcement with natural fibers as coir fibers are porous. Camphor ($C_6H_{16}O$) fresh carbon nanomaterial vendor and a natural source has both $sp^2$ and $sp^3$ covalent bonds with carbon while graphite which is a pure carbon has only $sp^2$ covalent bonds. As 0.1 g carbon nanotubes (CNT's) can be synthesized from 0.5 g of camphor it can be used to manufacture CNT's in large quantity. Camphor is a crystalline structure latex of Cinnamomum camphor tree which is environment-friendly and nontoxic [16]. Camphor soot can be used as reinforcement or coating on coir fibers to increase the thermal stability.

An attempt has been made from this perspective to enhance coir fibers thermal resistance by imparting the camphor soot particles into porous coir fibers through osmosis. As camphor soot is a burnt substance, it protects the lignocellulosic fibers at high temperatures. Thermal aspects and microstructure studies of coir fibers filled with camphor soot particles are discussed in this paper.

## Experimental

### Materials

Coir fibers were procured from SKT textile services India Pvt. Ltd. Their density was calculated using mass and volume of a bunch of fibers. The fibers volume was calculated by twisting coir fibers till an approximate cylinder was obtained. The apparent density of coir fibers was found to be 0.79 g/cm$^3$. Camphor soot was collected on a glass substrate by burning camphor tablets and apparent density of camphor soot was found to be 0.3 g/cm$^3$.

### Fabrication of Camphor Soot Reinforced Coir Fibers

Fabrication of camphor soot reinforced coir fibers was carried out through an osmosis process. Figure 1 shows modification of coir fibers which were, healthy and of uniform diameter and subjected to a prewash with distilled water. Moisture in the raw fibers was removed in a hot air oven at 50 °C for an hour, and their initial weight was recorded. They were then immersed in a camphor soot water solution prepared with the help of the ultra-sonication method and having different weight fractions (0.5, 1.0, and 1.5 wt. %) varied for different timespan and temperature intervals (4, 8 and 12 hrs.) and (30, 40 and 50 °C) respectively. The camphor soot solution with fibers was stirred thoroughly every two hours to reduce soot particles agglomeration as it enhances the camphor soot particles diffusion. During osmosis, camphor soot particles move from a higher concentration to one lower. Also, coir fibers are highly porous ranging between 22-30 %. Coir fiber surface has micropores measuring 4 μm approximately and the cross-section of a single fiber, of around 200 hollow elementary fibers has a diameter of 8-10 μm approximately while the lacuna at the center measures about 80 μm. Hence the fiber acts as a semi-permeable membrane in the solution leading to uniform infusion of camphor soot particles with an approximate size of 100-350 nm as revealed by the particle analyzer. This may be due to agglomeration of ~2-6 particles with weak van der walls forces between them. However as the results were not conclusive, the true particle size of camphor soot confirmed through use of a SEM micrograph, was found to be 40-50 nm. Keeping the ultimate tensile strength and RCSCF as objectives, the treatment was carried out according to $L_9$ orthogonal array with three levels for each parameter. The modified fibers were then taken out of the container and dried in a hot air oven to remove moisture. The final weight of the corresponding fibers was recorded.

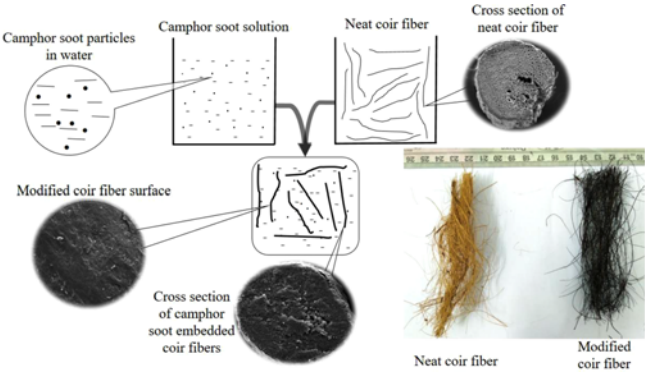


**Figure 1.** Modification of coir fibers through Osmosis.

### Characterization of Neat, Modified Coir Fibers and Camphor Soot

Tensile test was carried out according to ASTM D-3822, under ambient conditions using a kalpak computerized horizontal tensometer. Testing conditions maintained included a crosshead speed of 1 mm/min and load cell of 0.2 kN. Fiber diameter was 0.2 mm approximately; coir fibers were tested with a gauge length of 50 mm. The stated values are the average of a minimum of 5 measurements. The sample coir fiber preparation is shown in Figure 2. A healthy and equal diameter fibers were selected and glued to a paper frame to ensure that the fiber is aligned straight and is gripped

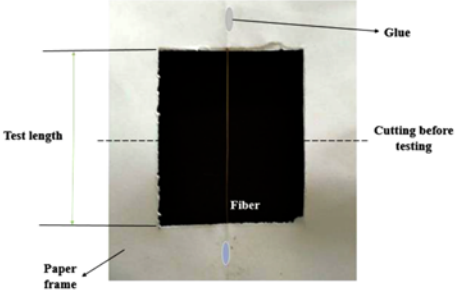


**Figure 2.** Paper frame for single fiber tensile test.

properly. Particle analysis of camphor soot was carried out using the Horiba laser scattering particle size distribution analyzer LA-960. XRD was performed using the PANalytical X'Pert Pro MPD using Cu-Kα radiation, scan angles (2θ) from 5 to 45 °, with a scanning speed of 2 ° $min^{-1}$, voltage of 40 kV and 30 mA current. FTIR spectroscopic measurements were carried out on neat and modified coir fibers with a Perkin Elmer-spectrum one FTIR Spectrometer. The spectral range was 4000-400 $cm^{-1}$ using a diamond ATR accessory and the DLATGS as detector.

TGA was conducted in an atmosphere containing nitrogen; the specimens were heated gradually from room temperature to 750 °C at a heating rate of 10 °C/min and nitrogen gas flow rate of 60 m*l*/min. Microstructure analysis was done through a scanning electron microscope; neat and modified coir fibers were sputtered with gold after osmosis and tested in a Tascam Vega 3 microscope with electron beam acceleration having 20 kV voltage.

## Results and Discussion

### Taguchi Design

The experiments were designed based on the Taguchi technique. The input process parameters used for manufacturing of CSRCF were temperature, time and camphor soot concentration. Control factors and levels are shown in Table 1. The objective functions chosen were ultimate tensile strength and RCSCF.

### Relative Camphor Soot in the Coir Fibers

Table 2 shows the initial and final weight of the fibers after osmosis. RCSCF for the modified fiber is calculated using equation (1). The results reveal that RCSCF of coir fibers for certain parameters was the highest at a temperature of 50 °C, time 12 hours and camphor soot concentration of 1.0 wt. %. This may be considered the optimal condition attributable to process parameters like time, temperature, and fiber porosity.

$$\text{RCSCF} = \frac{w_2 - w_1}{w_2} \times 100 \quad (1)$$

where $w_1$ and $w_2$ are the initial and final weights respectively.

**Table 1.** Control factors and levels

| Factors | Level 1 | Level 2 | Level 3 |
|---|---|---|---|
| Temperature (°C) | 30 | 40 | 50 |
| Time (min) | 4 | 8 | 12 |
| Camphor soot (wt. %) | 0.5 | 1.0 | 1.5 |

### Tensile Behaviour of Neat and Camphor Soot Reinforced Coir Fibers

Tensile behaviour of neat and modified coir fibers is shown in Figure 3. Neat and modified coir fibers are processed according to experimental design of the $L_9$ orthogonal array and stress-strain curves shown in Figure 4. There was a 37 % increase in tensile strength for CSRCF when compared to neat coir fibers. Neat coir fibers

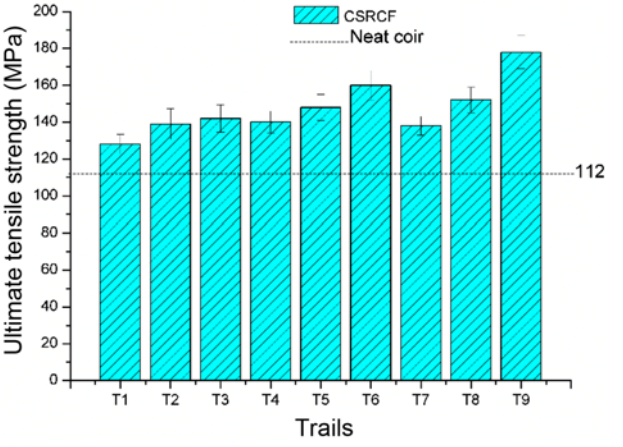


**Figure 3.** Variations in tensile strengths of both neat and modified coir fibers.

**Table 2.** Tensile strength and RCSCF of coir fibers

| Exp. run | Temp (°C) | Time (hrs.) | Conc. (wt. %) | Initial weight of coir fibers (g) | Final weight of coir fibers (g) | Weight of the camphor soot (g) | RCSCF (%) | CSRCF UTS (MPa) | Tensile strength neat coir (MPa) |
|---|---|---|---|---|---|---|---|---|---|
| 1 | 30 | 4 | 0.5 | 0.0694 | 0.0702 | 0.0008 | 1.13 | 128 | |
| 2 | 30 | 8 | 1.0 | 0.0759 | 0.0774 | 0.0015 | 1.96 | 139 | |
| 3 | 30 | 12 | 1.5 | 0.0713 | 0.0731 | 0.0018 | 2.46 | 142 | |
| 4 | 40 | 4 | 1.0 | 0.0720 | 0.0736 | 0.0016 | 2.17 | 140 | 112 |
| 5 | 40 | 8 | 1.5 | 0.0786 | 0.0806 | 0.0020 | 2.48 | 148 | |
| 6 | 40 | 12 | 0.5 | 0.0820 | 0.0838 | 0.0018 | 2.14 | 160 | |
| 7 | 50 | 4 | 1.5 | 0.0778 | 0.0798 | 0.0020 | 2.50 | 138 | |
| 8 | 50 | 8 | 0.5 | 0.0769 | 0.0789 | 0.0020 | 2.40 | 152 | |
| 9 | 50 | 12 | 1.0 | 0.0857 | 0.0889 | 0.0032 | 3.60 | 178 | |

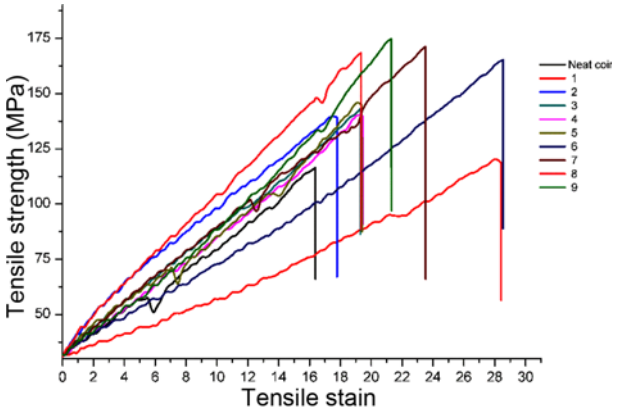


**Figure 4.** Stress-strain curves for both neat and modified coir fibers.

experienced delamination of elementary fibers during tension compared to CSRCF which could be due to catastrophic failure. CSRCF withstands more load as shown in Figure 3. The main reason for load-bearing capacity of modified fibers are high porosity and comprising elementary fibers filled with camphor soot particles during osmosis so that they became solid. On the other hand, coir fibers are very rich in lignin, a natural binding agent, which binds camphor soot particles firmly and decreases delamination of elementary fibers during tensile loads. Retting of coir fibers for longer periods could also be a reason for tensile strength increase.

## ANOVA Analysis of Modified Coir Fibers

ANOVA is a statistical method to measure the contribution

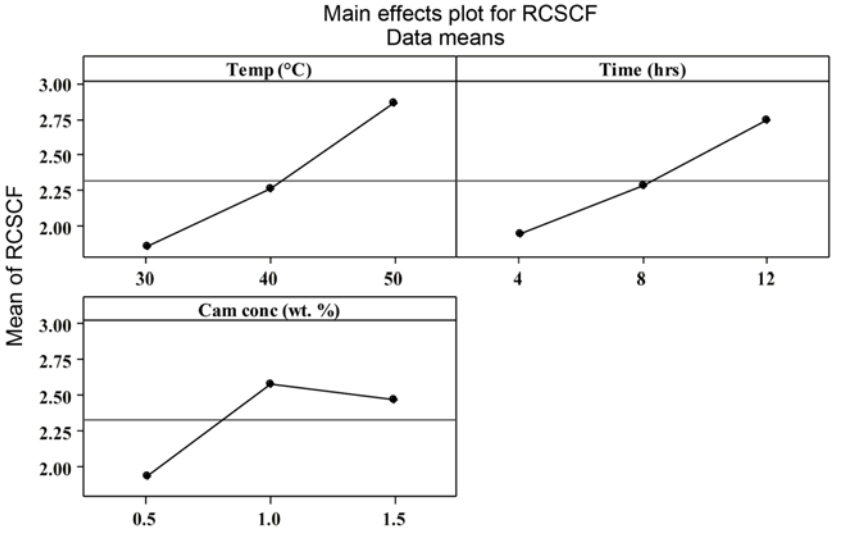


**Figure 5.** Main effects plot for RCSCF of coir fibers.

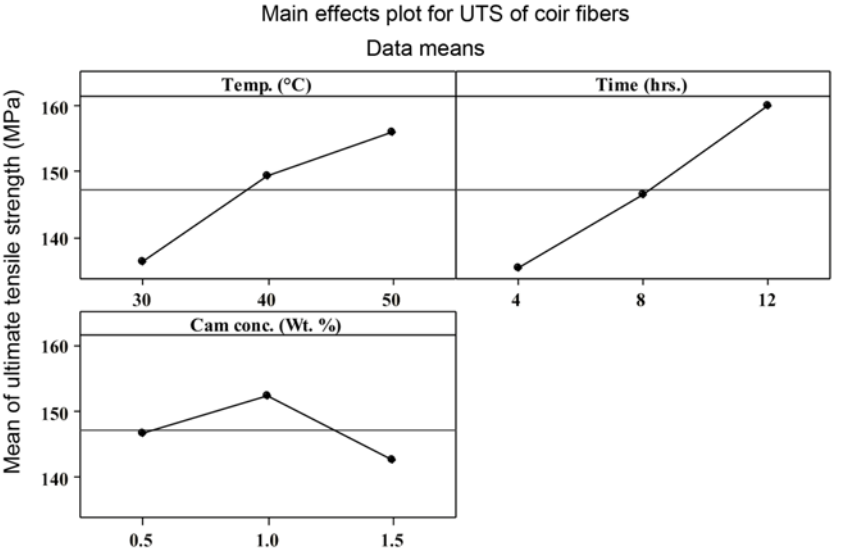


**Figure 6.** Main effects plot for the ultimate tensile strength of coir fibers.

**Table 3.** ANOVA for RCSCF of coir fibers

| Symbol | Factor | DOF | Sum of squares | Mean sum of squares | F | % Contribution |
|---|---|---|---|---|---|---|
| A | Temp | 2 | 1.57109 | 0.78554 | 31.83 | 47.304 |
| B | Time | 2 | 0.98249 | 0.49124 | 19.91 | 29.582 |
| C | Cam conc. | 2 | 0.71829 | 0.35914 | 14.55 | 21.627 |
| Error | | 2 | 0.04936 | 0.02468 | | |
| Total | | 8 | 3.32122 | | | |

**Table 4.** ANOVA for ultimate tensile strength of coir fibers

| Symbol | Factor | DOF | Sum of squares | Mean sum of squares | F | % Contribution |
|---|---|---|---|---|---|---|
| A | Temp | 2 | 600.22 | 300.11 | 7.74 | 34.583 |
| B | Time | 2 | 906.22 | 458.11 | 11.81 | 52.21 |
| C | Cam conc. | 2 | 141.56 | 70.78 | 1.83 | 8.15 |
| Error | | 2 | 77.56 | 38.78 | | |
| Total | | 8 | 1735.56 | | | |

of each parameter variation caused by the overall response variation. It is mainly used to locate the significance of input parameters. The latter include temperature, time and camphor soot concentration. ANOVA is calculated for RCSCF and ultimate tensile strength to analyse the importance of process parameters.

The main effect plot for RCSCF and ultimate tensile strength are shown in Figure 5 and 6 respectively which reveals that the optimal process parameters are the same for both RCSCF and ultimate tensile strength, i.e., $A_3B_3C_2$ which means, for a period of 12 hours at 50 $^{o}$C with 1 wt. % camphor soot concentration, our objectives seem to be achieved and can thus be considered optimum from the chosen set of parameters. This observation reveals that the RCSCF of the coir fibers is directly dependant on coir fibers ultimate tensile strength.

Table 3 reveals that temperature (47.3 %) greatly influences RCSCF enhancement followed by time (29.5 %), while camphor soot concentration (21.6 %) was the least influencing factor. Also, Table 4 which reveals use of ANOVA for ultimate tensile strength that time (52.2 %) was the most influencing factor followed by temperature while camphor soot concentration was the least influencing factor (8.1 %).

**Particle Analysis of Camphor Soot**

Figure 7 reveals the particle distribution of camphor soot, to study the distribution of camphor soot, dynamic light scattering (DLS) technique was used. The test was undertaken using HORIBA Scientific, LA-960 Laser Particle Size Analyser. It is inferred from the figure that camphor soot particles are in the cluster form, each of about 2-6 particles bonding together with a weak Van Der Waals force between them. However, the sample was kept in an ultra sonicator for one hour to uniformly distribute the particles in water. The particle distribution graph reveals a particle size between 100 nm to 350 nm due to the agglomeration of camphor soot particles. Moreover, the results from DLS were not conclusive and so SEM camphor soot micrograph was used

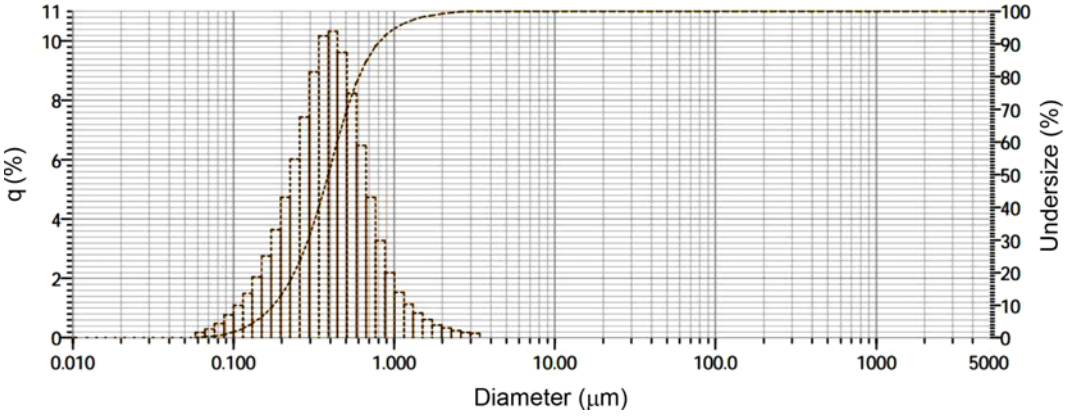


**Figure 7.** Particle analysis of camphor soot.

to confirm its particle size. It is seen that approximate particle size was between 40-50 nm.

**XRD Analysis of Camphor Soot and Camphor Soot Embedded Coir Fibers**

Figure 8 shows the X-ray diffraction pattern for neat coir fiber, CSRCF and camphor soot. Camphor soot reveals a strong and broadened peak at 2θ value 24.93 °, which corresponds to crystalline graphite (002) suggesting that carbon nanoparticles are formed from pyrolysis of camphor. Another weak peak at 2θ value of 41.36 °, corresponding to the (111) lattice plane shows the presence of amorphous graphite, and the results match earlier literature well [17,18].

Diffraction graphs for neat and CSRCF shows the effect of infusion of camphor soot particles in porous coir fibers clearly revealed by XRD. Crystalline cellulose components are embedded in the matrix of lignin, hemicellulose and pectin in raw fibers. During osmosis, the camphor soot particles are transmitted into hollow elementary fibers. Lignin as a natural binding agent binds camphor soot particles by changing fibers surface topography and their crystallographic structure. Further, the fibers modified surface ensures better compatibility with polymeric matrices as camphor soot particles are by nature hydrophobic.

The XRD graphs show two peaks; the first at a 2θ value of 7 and the other at 2θ value of 22 indicating that the fibers are semi-crystalline. This cellulose characteristic may be attributed to cellulose interaction between hydroxyl and carboxyl groups in the fiber's structure [19,20]. The diffraction graph for the neat coir fiber with a small peak at 2θ value of 8 revealed that as the fibers are semi-crystalline, the peak disappears in modified fibers due to the fibers processing in camphor soot solution at 50 °C for 12 hours raising camphor soot particle mantle to rise to the surface. The crystallinity index (CI) of neat and CSRCF were calculated using equation (2) and valued as 50.5 % and 49.86 % respectively. Crystallinity decreases marginally in CSRCF as camphor soot has amorphous graphite, the change in the fiber's surface topography after osmosis is the principal reason for a slight reduction in the crystallinity index [21,22].

$$CI = \frac{I_c - I_{am}}{I_c} \times 100 \quad (2)$$

where $I_c$ and $I_{am}$ are intensities of crystalline and amorphous peaks respectively.

**Thermogravimetric Analysis of Neat and Camphor Soot Imparted Coir Fiber**

Thermogravimetric Analysis (TGA) is method to inspect the thermal stability of lignocellulosic fibers. A typical TGA curve for natural fiber degradability reveals that specimen exposed to heat will gradually suffer mass loss; then the weight drops sharply over a narrow range and finally reverts to the zero slope as the sample gets exhausted. Figure 9 shows the typical TGA curves of coir fiber with or without camphor soot reinforcement. Three stages are seen during the degradation of natural fibers; in the first stage moisture and volatile compounds evaporate at 50-100 °C [23]. In the second stage, decomposition of hemicellulose occurs at approximately 200-300 °C [24]. In the last stage slight weight loss due to lignin and cellulose degradation is seen at temperatures of 400-500 °C [25]. It can be seen that the curve experiences two steps during degrading and that during the second step, thermal stability gradually increases as the hemicellulose is converted to char after the first stage. This could be the reason for thermal resistance which protects it against further degradation of lignin and cellulose. This is the main reason one witnesses the two-step degradation in natural fibers.

It is clear from the TGA curves that neat coir fibers,

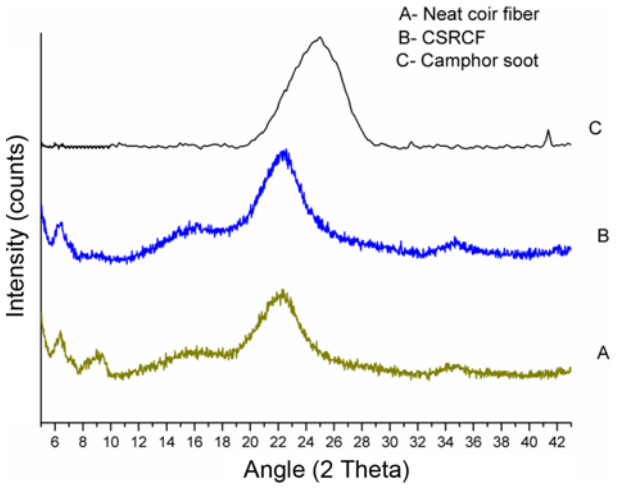


**Figure 8.** XRD variations for camphor soot and coir fibers with/ without camphor soot particles.

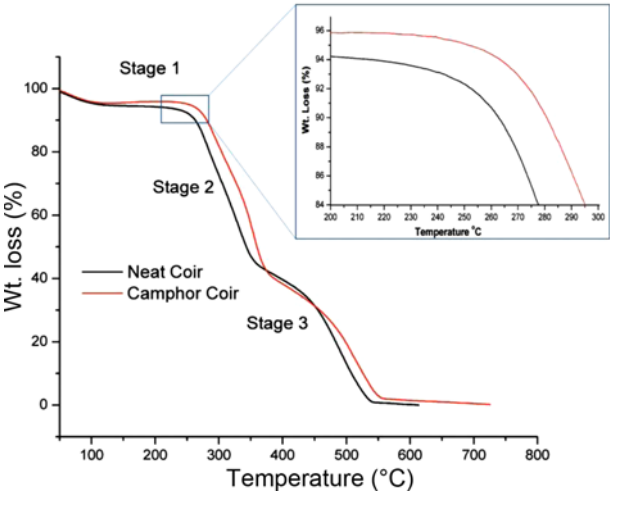


**Figure 9.** TGA analysis of neat and camphor soot reinforced coir fibers.

specially in stage two, start rapidly degrading at temperatures ranging from 220-230 °C. On the other hand. CSRCF showed considerable thermal stability between temperatures ranging between 260 °C and 270 °C which is a 15 % increase compared to neat fibers thereby revealing that camphor soot particles degrade at high temperatures. Such camphor soot embedded coir fibers can be used as reinforcement in high-temperature polymers like nylon.

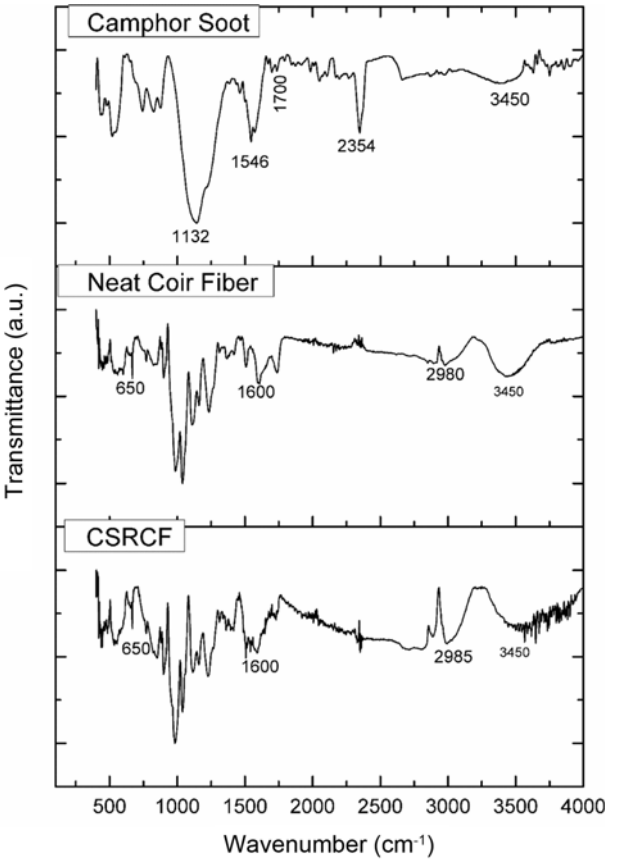


**Figure 10.** FTIR plots for camphor soot and coir fibers with/ without camphor soot particles.

## FTIR Analysis of Neat and Modified Coir Fibers

FT-IR spectroscopy analysis studied the effect of camphor soot infusion into porous coir fibers. Figure 10 shows IR spectra in the 4000-400 $cm^{-1}$ range. FT-IR spectra of neat, CSRCF and camphor soot show differences in the peaks of lignocellulosic fibers. The absorption band at 3450 $cm^{-1}$ relates to the O-H stretching vibration characteristic and the hydrogen bond of the hydroxyl groups [26] as seen in neat coir fibers, but CSRCF has a diminished peak which could be due to fiber surface being covered by camphor soot particles. Camphor soot had a peak at 3450 $cm^{-1}$ corresponding to OH stretching (H-bonded) from the alcoholic group in camphor soot. The band at 2980 $cm^{-1}$ is a characteristic for C-H stretching vibration from CH and $CH_2$ in cellulose and hemicellulose components [27,28]. Slightly drifted peaks in this band for modified coir fibers may be attributed to the formation of $SP^2$ bonds with cellulose and hemicellulose components, whereas in camphor soot, the spectrum peak is near 2354 $cm^{-1}$ due to C≡C bonds. The peak of 1600 $cm^{-1}$ refers to carboxylic ester in hemicellulose, pectin, and wax [28]. The peaks disappear after camphor soot embedment in coir fibers. The camphor soot peak around 1132 $cm^{-1}$ is related to (C-O), 1700 $cm^{-1}$ & 1546 $cm^{-1}$ and corresponds to carbonyl (C=O) stretching and (C-C) stretching respectively [18]. The peak around 650 $cm^{-1}$ matches the presence of lignin. Neat coir fibers have a higher peak compared to camphor soot infused fibers. This could be due to the coating of camphor soot particles on the fiber's surface as lignin is a natural binder, and due to particles embedded fibers due to the latter's porosity.

## Morphology of Neat and Camphor Soot Infused Coir Fibers

Figure 11(a-h) shows the morphology of coir fibers with

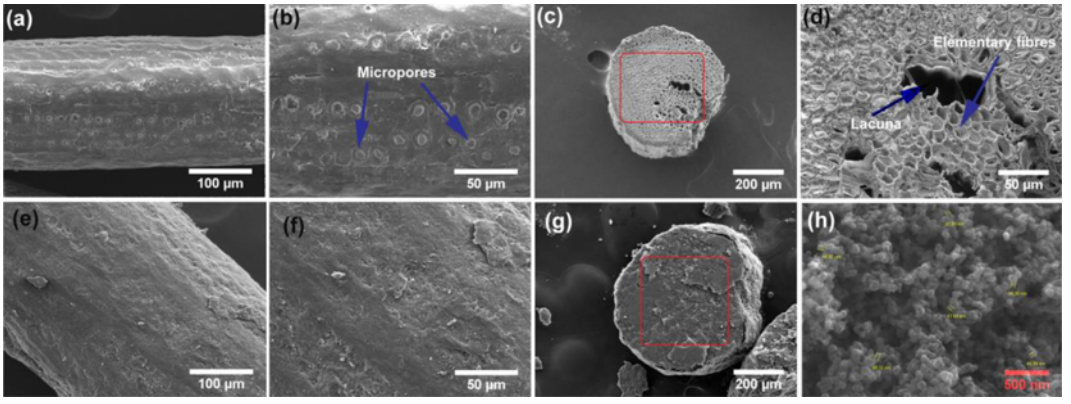


**Figure 11.** SEM images of neat and camphor soot embedded coir fibers, (a) neat coir fiber, (b) micropores on neat coir fiber, (c) C/s of neat coir fiber, (d) magnified neat coir fiber C/s, (e) camphor soot embedded coir fiber, (f) magnified CSRCF, (g) C/s of camphor soot reinforced coir fiber, and (h) camphor soot.

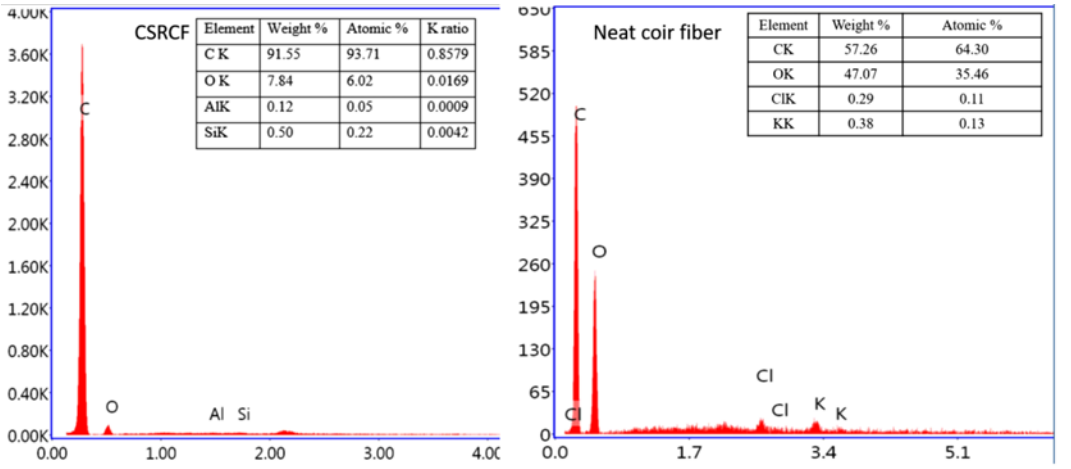


**Figure 12.** EDS data of cross sections of neat and camphor soot infused coir fiber.

and without camphor soot particles and camphor soot. It is seen from Figure 11(a) and (b) that neat coir fibers are highly porous as their surfaces are full of micropores. Figure 11(c) and (d) are a cross section of neat coir fibers which reveal the extent of fibers porosity. It is made up of a bunch of fibers called elementary fibers with a lacuna at the center. Figure 11(e) and (f) show that micropores are filled with camphor soot particles with the surface being smooth compared to neat fibers. High lignin content in coir fiber has a major role in binding the camphor soot particles firmly. Figure 11(g) is a micrograph of the cross section of a camphor soot-filled coir fiber. Figure 11(f) is a highly magnified image of camphor soot where, soot particles are spherical and measures 40-50 nm approximately. They are bonded with weak Van der Waals forces. It is clear from the SEM micrograph that camphor soot is not porous. Figure 12 shows the EDS data of neat and CSRCF C/s as is evident from the morphology; it is seen that the highly porous coir fiber's cross-section is filled with camphor soot particles. The EDS result for neat fiber contains 64 % carbon, 35 % oxygen and traces of chlorine and potassium. But camphor soot-filled coir fiber has 95.44 % carbon, 4.41 % oxygen, 0.05 % aluminum and 0.10 % silicon. It is clear from the results that camphor soot embedded in coir fibers can protect them from thermal degradation.

## Conclusion

To enhance coir fibers tensile and thermal stability, we investigated the effect of interfacial alterations on coir fibers by infusing camphor soot particles through osmosis using the Taguchi technique. The following conclusions can be drawn.

1. ANOVA results revealed the optimal level of process parameters as $A_3B_3C_2$ in the table which reveals a temperature of 50 °C, 12 hours time and camphor soot concentration of 1 wt. %. These parameters enhanced tensile strength and RCSCF.
2. Tensile strength of CSRCF increased after addition of camphor soot particles by about 37 % compared neat fibers.
3. XRD analysis revealed that camphor soot embedded coir fibers had a marginal decrease in the crystallinity index after camphor soot infusion.
4. Thermogravimetric analysis of camphor soot embedded fibers showed considerable increase in thermal stability, which is nearly 15 % compared to neat coir fibers.
5. FTIR results revealed that the OH- peak tended to diminish after reinforcement of camphor soot in neat fibers. It also lowered CH stretching and carbonyl groups peaks.
6. SEM morphology revealed that, coir fibers are embedded with camphor soot particles. EDS results show a 94 % carbon presence in the camphor soot in the cross-section of coir fibers compared to neat fiber's cross-section with around 64 % of carbon.

## References

1. K. Rohit and S. Dixit, *Polym. Renew. Resour.*, **7**, 43 (2016).
2. N. Ayrilmis, S. Jarusombuti, V. Fueangviva, P. Bauchongkol, and R. H. White, *Fiber. Polym.*, **12**, 919 (2011).
3. A. K. Mohanty, M. Misra, and G. Hinrichsen, *Macromol. Mater. Eng.*, **276**, 1 (2000).
4. L. Q. N. Tran, T. N. Minh, C. A. Fuentes, T. T. Chi, A. W. Van Vuure, and I. Verpoest, *Ind. Crops Prod.*, **65**, 437 (2015).
5. J. R. Araujo, W. R. Waldman, and M. A. De Paoli, *Polym. Degrad. Stabil.*, **93**, 1770 (2008).
6. Y. Xie, C. A. Hill, Z. Xiao, H. Militz, and C. Mai, *Compos. Pt. A-Appl. Sci. Manuf.*, **41**, 806 (2010).
7. M. N. Belgacem and A. Gandini, *Compos. Interfaces*, **12**,

41 (2005).
8. T. D. Hapuarachchi and T. Peijs, *Compos. Pt. A-Appl. Sci. Manuf.*, **41**, 954 (2010).
9. P. Zadorecki and K. B. Abbas, *Polym. Compos.*, **6**, 162 (1985).
10. C. Klason, J. Kubat, and H. E. Stromvall, *Int. J. Polym. Mater.,* **10**, 159 (1984).
11. M. Misra, A. K. Mohanty, P. Tummala, and L. T. Drzal, *In ANTEC Conference Proceedings*, **2**, 1603 (2004).
12. Z. N. Azwa, B. F. Yousif, A. C. Manalo, and W. Karunasena, *Mater Des.*, **47**, 424 (2013).
13. M. J. John and R. D. Anandjiwala, *Polym. Compos*., **29**, 187 (2008).
14. R. Kozłowski and M. Władyka-Przybylak, *Polym. Adv. Technol.,* **19**, 446 (2008).
15. D. B. Dittenber and H. V. GangaRao, *Compos. Pt. A-Appl. Sci. Manuf.*, **43**, 1419 (2012).
16. M. Kumar and Y. Ando, *Dimond*. *Relat. Mater.*, **12**, 998 (2003).
17. M. S. Swapna and S. Sankararaman, *Int. J. Mater. Sci.*, **12**, 541 (2017).
18. B. N. Sahoo and B. Kandasubramanian, *RSC Adv.*, **4**, 11331 (2014).
19. J. Jayaramudu, B. R. Guduri, and A. V. Rajulu, *Carbohydr. Polym*., **79**, 847 (2010).
20. V. S. Sreenivasan, S. Somasundaram, D. Ravindran, V. Manikandan, and R. Narayanasamy, *Mater. Des.,* **32**, 453 (2011).
21. S. Park, J. O. Baker, M. E. Himmel, P. A. Parilla, and D. K. Johnson, *Biotechn. Biofuels,* **3**, 10 (2010).
22. M. K. Rambo and M. Ferreira, *J. Brazil Chem. Soc.*, **26**, 1491 (2015).
23. P. Methacanon, U. Weerawatsophon, N. Sumransin, C. Prahsarn, and D. T. Bergado, *Carbohydr. Polym*., **82**, 1090 (2010).
24. L. B. Manfredi, E. S. Rodríguez, M. Wladyka-Przybylak, and A. Vázquez, *Polym. Degrad. Stabil.,* **91**, 255 (2006).
25. S. H. Lee and S. Wang, *Compos. Pt. A-Appl. Sci. Manuf.,* **37**, 80 (2006).
26. M. A. Spinace, C. S. Lambert, K. K. Fermoselli, and M. A. De Paoli, *Carbohydr. Polym*., **77**, 47 (2009).
27. H. Essabir, E. Hilali, A. Elgharad, H. El Minor, A. Imad, A. Elamraoui, and O. Al Gaoudi, *Mater. Des*., **49**, 442 (2013).
28. F. D. Ardejani, K. Badii, N. Y. Limaee, S. Z. Shafaei, and A. R. Mirhabibi, *J. Hazard Mater.*, **151**, 730 (2008).